PAPER REFERENCE: 9.257

EFFECTS OF DIFFUSE CRACKING AROUND A COHESIVE CRACK

I. Arbilla, J. Planas, G.V. Guinea and M. Elices

Departamento de Ciencia de Materiales, Universidad Politécnica de Madrid,
ETS de Ingenieros de Caminos, Ciudad Universitaria s/n, 28040 Madrid, Spain

ABSTRACT

The cohesive crack model is a relatively simple and accurate means of describing fracture in concrete and other quasibrittle materials. In its standard application, it is assumed that all the material surrounding the cohesive crack remains linear elastic, but detailed analyses show that the tensile strength is exceeded within the supposedly elastic region, which means that secondary cracking must occur. This paper describes a simple extension of the cohesive crack to include secondary cracking, and discusses the results of its application to three-point-bend test specimens.

INTRODUCTION

The cohesive crack model, first proposed by Barenblatt and Dugdale [1,2] in very specific contexts, was later extended by Hillerborg [3] to become a general approach to the fracture of concrete in tension. The model has proved to be relatively simple and efficient to describe the fracture of concrete and other quasibrittle materials, at least in the cases where failure occurs through a single crack or a set of discrete cracks.

One of the simplifications usually included in the cohesive crack model is that all nonlinear behavior is localized in the cohesive zone while the material surrounding the crack remains linear elastic. Although this hypothesis is not conceptually necessary [4,5], it simplifies both theoretical and numerical analyses of cohesive crack problems and has become a basic ingredient of the standard formulation.

A limitation of the standard formulation of the cohesive crack model is that it leads to solutions that contradict one of the basic hypotheses of the model, namely, that a cohesive crack forms in at a formerly elastic point when the stress reaches the tensile strength f_t. Indeed, in most of the solutions of single cohesive crack problems, more or less large regions have been found in the supposedly elastic bulk material where the tensile strength is exceeded. For example, as shown in Figure 1, a small but finite region over which the largest principal stress exceeds the tensile strength is found around the cohesive crack tip in a three-point-bend specimen in which a cohesive crack is made to grow in mode I from a relatively deep notch [6,7]. For unnotched thee-point-bend specimens it has long been suggested that the standard solution involved stresses exceeding the tensile strength over allegedly elastic regions [8], as quantitatively demonstrated by Olsen [9] some of whose results are compiled in Figure 2, which shows large areas over which the tensile strength is exceeded.

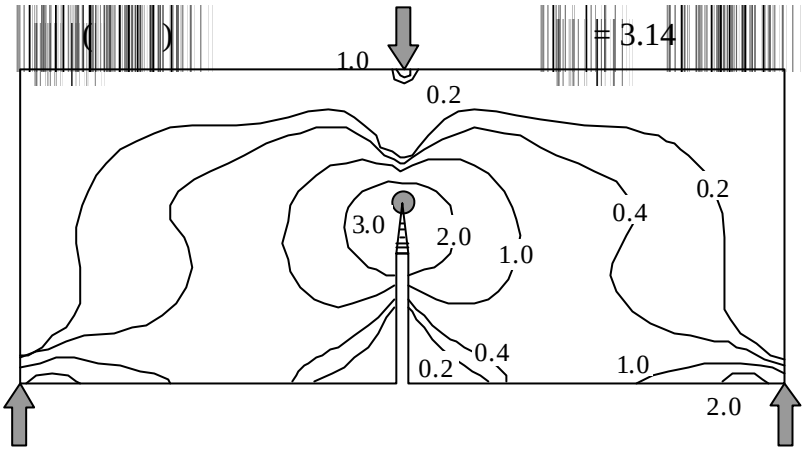

Figure 1: Isolines of maximum principal stress at peak load for a three-point-bend notched beam. The tensile strength f_t is exceeded over a small region around the cohesive crack tip. (Adapted from [7].)

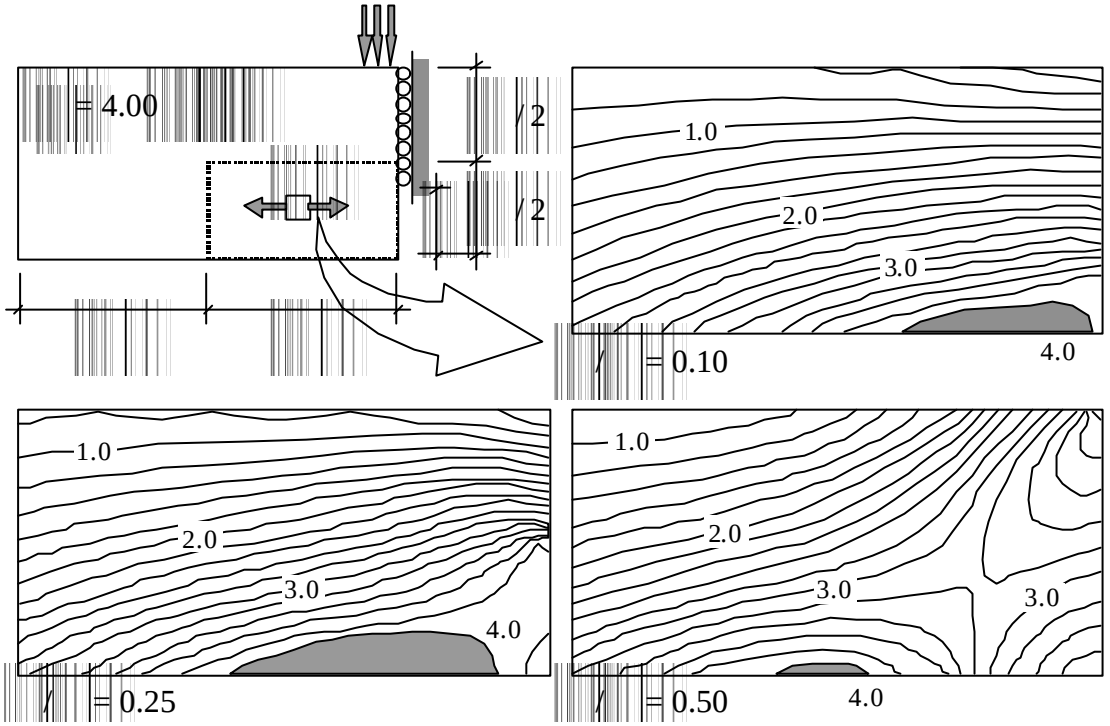

Figure 2: Isolines of horizontal normal stress for a three-point-bend unnotched beam for various relative depths *a/D* of the cohesive zone . The tensile strength f_t is exceeded over the gray shadowed regions. (Adapted from [9].)

The foregoing facts imply the following 3 consequences:

1. The standard approach to the cohesive crack model leads to inconsistent solutions whose accuracy needs to be assessed through a higher level model.

2. According to the cohesive crack model itself, secondary cracking must occur in the regions where the tensile strength is exceeded.

3. A higher-order model is needed that, while preserving the main concepts of the cohesive crack model, eliminates the inconsistency and adequately describes the secondary cracking.

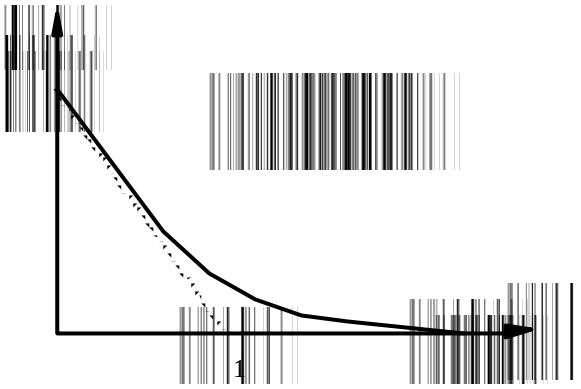

Figure 3: Generic softening stress-crack opening curve.

This work presents one of the many possible higher-order models and describes the results of its application to the three-point-bend unnotched beam. The model has the advantages of being conceptually and formally simple, and of using only concepts coming from the cohesive crack itself.

DIFFUSE CRACK MODEL

The diffuse crack model developed in this work is a three-dimensional generalization of the unidimensional model proposed by Planas and Elices to describe shrinkage microcracking in concrete [10]. The basic ingredient of the model is the cohesive crack, which is assumed to form perpendicular to the maximum principal stress when this reaches the tensile strength f_t. After the cohesive crack has formed, the stress transferred across its faces is assumed to be given, for *monotonic* mode I crack opening, by a unique function of the crack opening w:

$$s = f(w) \tag{1}$$

where $f(w)$ is usually known as the softening function and (for concrete) has the shape depicted in Figure 3.

To build the diffuse crack model we use the basic cohesive crack model just described together with some simple complementary assumptions regarding crack kinematics. For simplicity, we first describe the uniaxial model and then give the generalization to three dimensions.

Uniaxial Model

The basic idea in the uniaxial model is that diffuse cracking can be described as an array of parallel cohesive cracks, spaced at a relatively small distance s, in an otherwise elastic bar. If the cracks are close enough, we can describe their macroscopic effect as a distributed inelastic strain e^p given by

$$e^p = \frac{w}{s} \tag{2}$$

where w is the average crack opening.

The uniaxial stress transferred through the crack array for monotonic inelastic stretching, directly derives from the softening curve (1) as

$$s = f(se^p) = f_s(e^p) \tag{3}$$

where $f_s(e^p)$ is a stress-inelastic strain curve which displays softening. However, if the crack spacing is small, the softening rate tends to vanish, and the model displays perfectly plastic behavior. Indeed, for a softening curve such

as that in Figure 3, with an initial trend approximately linear, defined by the horizontal intercept w_1, the softening or stress drop Δs is given by

$$\Delta s = f_t \frac{s}{w_1} e^p \tag{4}$$

Hence, for infinitely close cracks, s vanishes and so does Δs. Therefore, as far as monotonic stretching is concerned, the behavior tends to perfectly plastic as the crack spacing is reduced.

To complete the model, we need to specify the unloading behavior because eventually a main cohesive crack will develop, and as it grows, the zone of diffuse cracking may unload. Planas and Elices [10, with the results of other authors [11,12],] justified that when a crack opens only slightly it does not close again upon unloading. We adopt here this point of view and assume that the inelastic strain e^p is fully irrecoverable. This is formally identical to assuming an elastic-plastic stress-strain behavior. The behavior is perfectly plastic if $s = 0$, and is plastic with softening if $s \neq 0$.

Triaxial Model

The simplest way to generalize the former uniaxial model to three dimensions is to assume an elastoplastic behavior with a Rankine criterion and associative flow rule. The corresponding equations are

$$\boldsymbol{s} = \boldsymbol{E}(\boldsymbol{e} - \boldsymbol{e}^p) \tag{5}$$

$$s_I - f_s(\tilde{e}^p) = 0 \tag{6}$$

$$d\boldsymbol{e}^p = \mathbf{P}_I \, d\tilde{e}^p \tag{7}$$

where $\boldsymbol{s}$ is the stress tensor, $\boldsymbol{E}$ the fourth-order elastic tensor, $\boldsymbol{e}$ the strain tensor, $\boldsymbol{e}^p$ the inelastic strain tensor, s_I the maximum principal stress, $\tilde{e}^p$ the equivalent inelastic strain, and $\mathbf{P}_I$ the projector of $\boldsymbol{s}$ in the direction of its first principal stress. The function $f_s(\tilde{e}^p)$ is identical to that defined for the uniaxial model, by equation (3).

NUMERICAL ANALYSIS

The model just described was applied to analyze the influence of diffuse cracking on the predicted behavior of unnotched three-point-bend beams. Geometrically similar beams were analyzed with a span-to-depth ratio of four. Five beam depths were considered, scaled according to the ratios 1:2:4:8:16. Three calculations were made for each beam depth:

1. Standard cohesive crack model: main cohesive crack running through elastic material.
2. Nonsoftening diffuse cracking: main cohesive crack running through a material with (potentially) infinitely close diffuse cracks (crack spacing $s = 0$).
3. Softening diffuse cracking: main cohesive crack running through a material with diffuse softening cracks corresponding to an assumed minimum crack spacing identical to the finite element size ($s = D/64$, where D is the beam depth).

The softening curve used in all the calculations (the only material property required apart from elastic constants) is shown in Figure 4. This corresponds to an actual microconcrete tested in the authors' laboratory.

The numerical simulations were carried out using ABAQUS. Softening spring elements located along the central cross section simulated the main crack. The surrounding material was simulated through a user-defined routine (UMAT) implementing the model defined in the previous section (none of the finite element codes accessible to the authors implement a Rankine plastic criterion with associative flow rule).

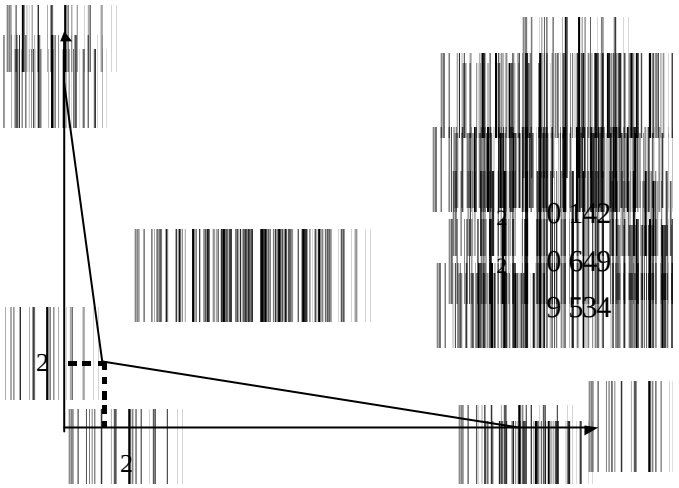

Figure 4: Softening curve used in the computations

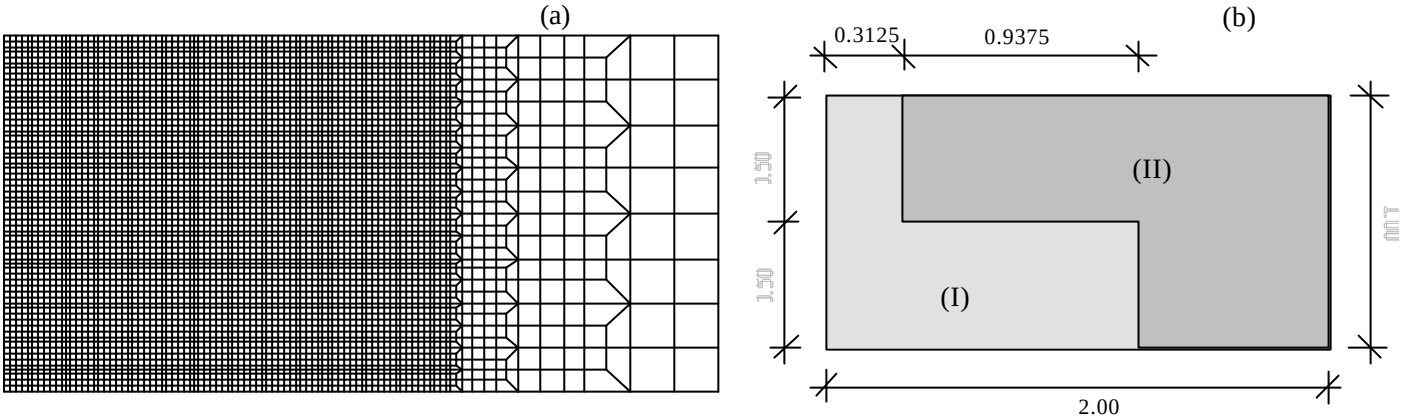

Figure 5: Numerical modeling: (a) finite element mesh over the right half-specimen, (b) domain subdivision—I for normal elements and II superelement.

The finite element mesh used to model the right half of the specimen is shown in Figure 5, together with the definition of the elastic superelement used to speed up the calculations, which were driven in arc-length control, and were free of problems for the standard cohesive crack model. When diffuse cracking was included, the convergence rate was slower, and problems arose in continuing the calculation for large specimens where strong snap-back was present, particularly for the diffuse cracking with softening. Spontaneous unloading sometimes occurred, which required direct intervention of the operator (stopping just before unloading and restarting the calculation using the saved results and a different loading step).

RESULTS

The results are shown in dimensionless form, so they are useful not only for the particular microconcrete considered here, but also for any other material with a softening function of identical shape. In particular, the dimensionless size of the specimen is obtained by dividing the depth of the specimen D by the characteristic length l_{ch} defined as

$$l_{ch} = \frac{EG_F}{f_t^2} \tag{8}$$

where E is the elastic modulus. The value of the characteristic length of the microconcrete was l_{ch} = 122 mm,. while for an ordinary concrete $l_{ch} \approx 300$ mm.

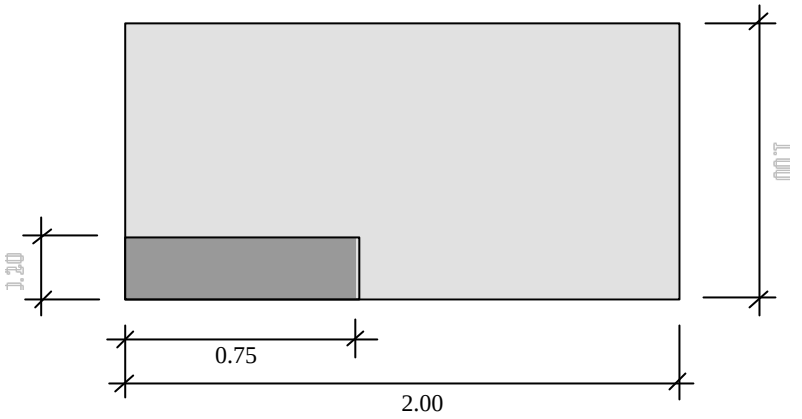

Figure 6: Right half of the specimen; the dark rectangle shows the zone, magnified in the following figure, where diffuse cracking takes place. All dimensions are referred to the beam depth.

One of the main results is that the diffuse crack model relieves the overstress appearing in the standard cohesive crack approach, so the stress nowhere exceeds the tensile stress. Of course, this is done at the expense of inelastic strains appearing in the material. The inelastic strain concentrates in the small dark rectangle shown in Figure 6, and its distribution inside that rectangle is shown in Figure 7 for various cases. For nonsoftening diffuse cracking, the inelastic strain is smoothly distributed, and is more intense for small sizes (7a) than for large sizes (Figure 7b). For softening diffuse cracking the inelastic strain is again more intense for small sizes (Figure 7c) than for large sizes (Figure 7d), the distribution being less smooth and with localization bands that may be identified in small sizes (Figure 7c). This is the main difference between the two diffuse crack models.

The first consequence of the localization is that the maximum inelastic strain is about 5 times larger in the softening diffuse cracks. This is shown in Figure 8a together with the influence of the beam depth. Although the existence of localization bands is numerically significant, its effect on the experimental results is nil. In fact, the softening associated with the worst strain localization is shown in Figure 8b and is less than 0.4% of f_t for all the investigated sizes. The corresponding (maximum) crack opening is $w \approx 0.003 G_F / f_t \approx 0.1 \mu m$ for a typical concrete with $G_F = 100\,\text{N/m}$ and $f_t = 3\,\text{MPa}$. This means that the localization bands, which could be seen as isolated cracks, are virtually impossible to detect experimentally since their opening is in the submicron range.

Figure 9 shows the load-displacement curves for two beam depths calculated in the three ways defined in the previous section. The effect of including diffuse cracking is seen to be marginal. In particular, the influence on the peak load never exceeds 1.2% of the value computed by the standard method

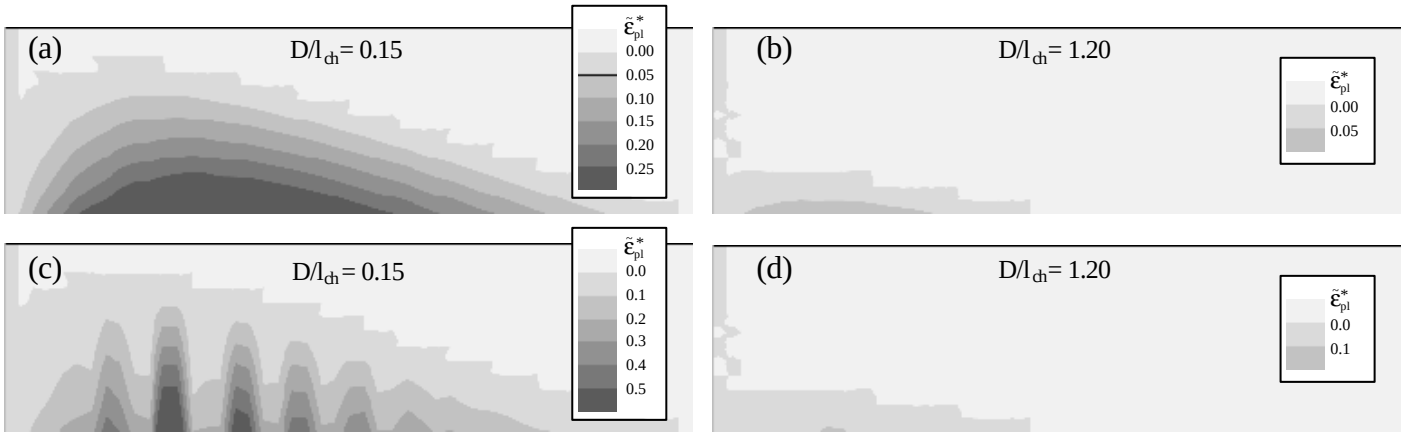

Figure 7: Inelastic strain distributions for diffuse cracking: (a) and (b) nonsoftening; (c) and (d) softening. The parameter $\tilde{e}^*_{pl} = \tilde{e}^p E / f_t$ is the equivalent elastic strain referred the elastic uniaxial strain at peak stress.

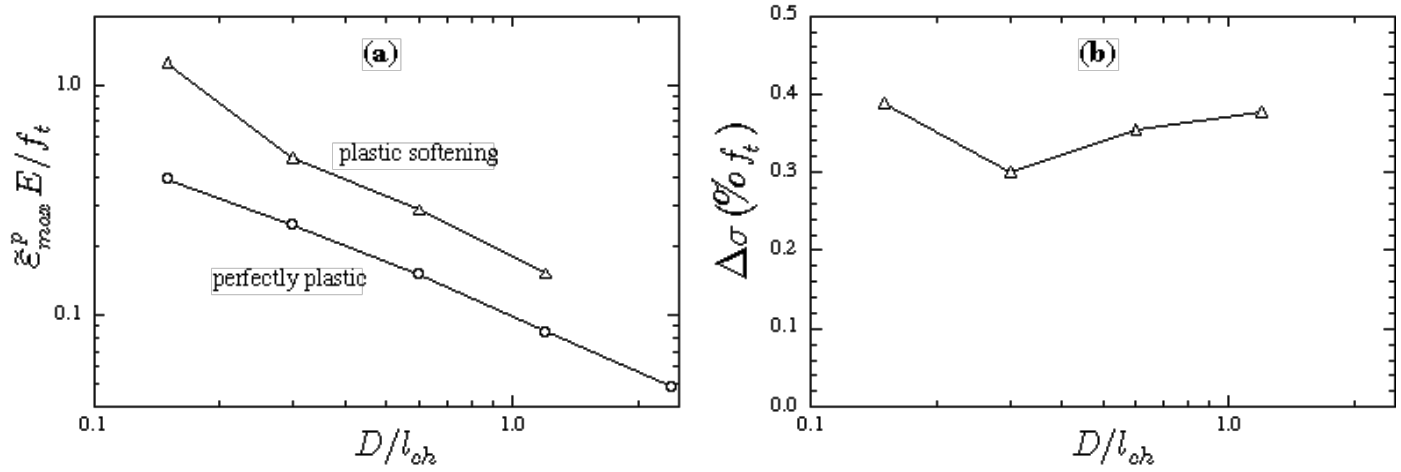

Figure 8: Size effect on inelastic strain localization: (a) maximum inelastic strain versus beam depth for the two models of diffuse cracking, and (b) maximum amount of softening occurring in the diffuse cracks versus beam depth.

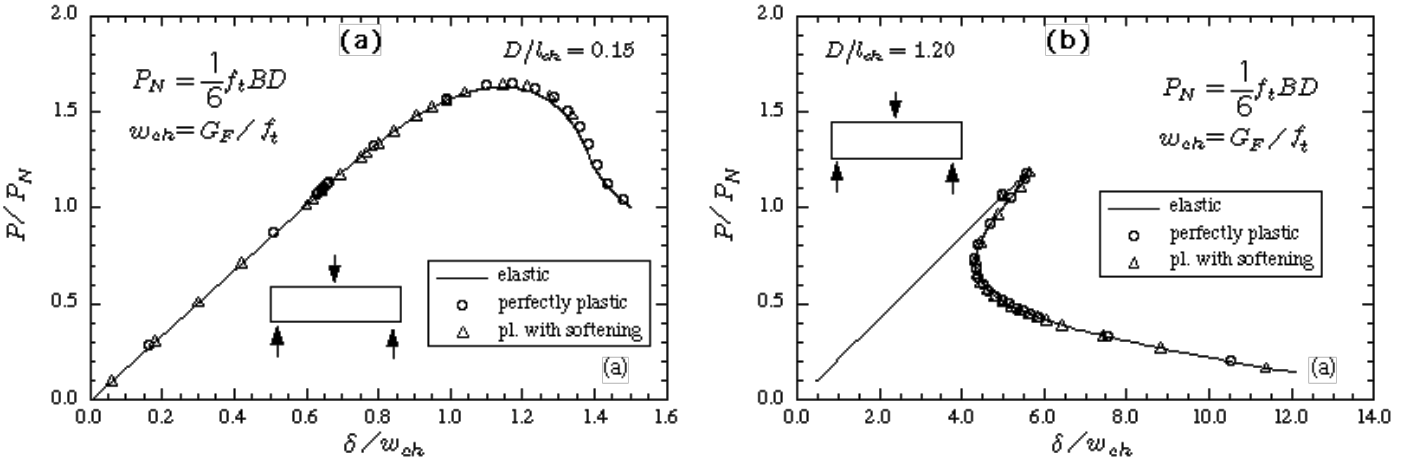

Figure 9: Comparison of load-displacement curves computed according to the three models: (a) for $D/l_{ch} = 0.15$; and (b) for $D/l_{ch} = 1.20$.

CONCLUSIONS

- Both versions of the diffuse crack model described here (nonsoftening and softening) seem to be adequate to eliminate the inconsistency of the standard cohesive crack model and to describe secondary cracking that must necessarily occur in specimens and structures failing through a single main crack.

- Although the softening version of the model shows localization at a numerical level, its influence on the mechanical response is negligible and the localizations are impossible to detect experimentally since they correspond to localized displacement jumps of the order of tenths of a micron.

- Since in the softening version of the model some degree of arbitrariness is present (only one crack per element is allowed and the size of the element is arbitrary) we suggest using the nonsoftening version unless there is evidence against this (e.g. if a localization of secondary cracking is known to exist).

- One situation where multiple cracking is known to exist is that of cracking induced by shrinkage or thermal gradients. In such cases, the softening version of the model can be used to follow the evolution of diffuse cracking as well as of main cracks (a main crack would be represented, then, as a *crack band*).

- For three-point-bend unnotched beams, the mechanical response is affected only slightly by the secondary cracking. The standard model (which is simpler and faster) can thus be used for most practical purposes

REFERENCES

1. Barenblatt, G. I. (1962). *Adv. Appl. Mech.* **7**, 55.
2. Dugdale, D. S. (1960) *J. Mech. Phys. Solids* 8, 100.
3. Hillerborg, A., Modéer, M. and Petersson, P.-E. (1976)
4. Elices, M. and Planas, J. (1989). In: *Fracture Mechanics of Concrete Structures*, pp. 16–66, Elfgren, L. (Ed). Chapman and Hall, London.
5. Bazant, Z.P. and Planas, J. (1998). *Fracture and Size Effect in Concrete and Other Quasibrittle Materials*. CRC Press LLC, Boca Ratón, Florida.
6. Guinea, G.V. (1990) *Medida de la Energía de Fractura del Hormigón*. PhD thesis, Universidad Politécnica de Madrid, Spain.
7. Planas, J., Elices, M., and Guinea, G.V. (1992). *Materials and Structures* **25**, 305.
8. Olsen, P.C. (1994). *Magazine of Concrete Research* **46**(168), 209.
9. Gustafsson, P.J. (1985). *Fracture Mechanics Studies of Non-Yielding Materials Like Concrete: Modeling of Tensile Fracture and Applied Strength Analyses*. Report No. TVBM-1007, Division of Building Materials, Lund Institute of Technology, Lund, Sweden.
10. Planas, J. and Elices, M. (1993). In: *Creep and Shrinkage of Concrete*, pp. 357–368, Bazant, Z.P. and Carol, I. (Eds). E \& FN Spon, London.
11. Reinhardt, H.W. (1984) *Heron* **29**(2), 3.
12. Yankelevsky, D.Z. and Reinhardt, H.W. (1987) *ACI Materials Journal* **84**(5), 365.